
Article:
Chance, Rosemary Jane orcid.org/0000-0002-5906-176X, Hamilton, Jacqueline Fiona orcid.org/0000-0003-0975-4311, Carpenter, Lucy Jane orcid.org/0000-0002-6257-3950 et al. (3 more authors) (2018) Water-Soluble Organic Composition of the Arctic Sea Surface Microlayer and Association with Ice Nucleation Ability. Critical Reviews in Environmental Science and Technology. pp. 1817-1826. ISSN 1547-6537

https://doi.org/10.1021/acs.est.7b04072

Water-soluble organic composition of the Arctic sea surface microlayer and association with ice nucleation ability

Rosie J. Chance[*1], Jacqueline F. Hamilton[1], Lucy J. Carpenter[1], Sina C. Hackenberg[1], Stephen J. Andrews[1], Theodore W. Wilson[2†]*

1. Wolfson Atmospheric Chemistry Laboratories, Department of Chemistry, University of York, Heslington, York, YO10 5DD, UK.
2. School of Earth and Environment, University of Leeds, Woodhouse Lane, Leeds, LS2 9TJ, UK.

†Now at Owlstone Medical Ltd., 162 Cambridge Science Park, Milton Road Cambridge, CB4 0GH, UK.

* Corresponding author: rosie.chance@york.ac.uk

Abstract

Organic matter in the sea surface microlayer (SML) may be transferred to the atmosphere as sea spray and hence influence the composition and properties of marine aerosol. Recent work has demonstrated that the SML contains material capable of heterogeneously nucleating ice, but the nature of this material remains largely unknown. Water-soluble organic matter was extracted from SML and underlying seawater from the Arctic and analyzed using a combination of mass spectrometric approaches. High performance liquid chromatography-ion trap mass spectrometry (LC-IT-MS), and Fourier transform ion cyclotron resonance MS (FT-ICR-MS), showed seawater extracts to be compositionally similar across all stations, while microlayer extracts had a different and more variable composition. LC-IT-MS demonstrated the enrichment of particular ions in the microlayer. Ice nucleation ability (defined as the median droplet freezing temperature) appeared to be related to the relative abundances of some ions, although the extracts themselves did not retain this property. Molecular formulae were assigned using LC - quadrupole time-of-flight MS (LC-TOF-MS^2) and FT-ICR-MS. The ice nucleation tracer ions were associated with elevated biogenic trace gases, and were also observed in atmospheric aerosol collected during the summer, but not early spring suggesting a biogenic source of ice nuclei in the Arctic microlayer.

39

40 **TOC/Abstract art**

41 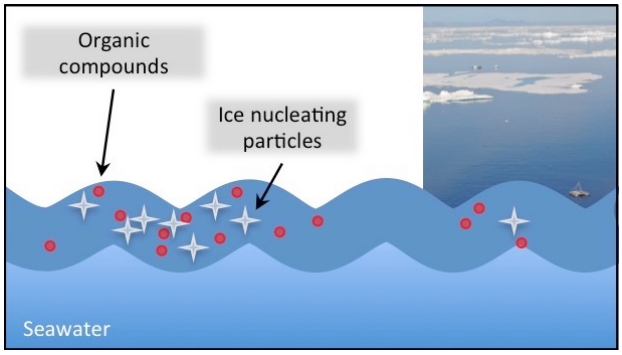

Introduction

The sea surface microlayer (SML) is a thin layer of water at the sea-air interface in which chemical, physical and biological properties differ from those of the underlying seawater[1]. The SML has an operationally defined thickness of ~1 to ~1000 μm [1], and surfactant enrichments have been found to persist up to wind speeds of up to at least ~ 13 m s^{-1} [2, 3]. It has been recognized as a distinct compartment for photochemical reactions[4, 5] and biogeochemical transformations[1].

As the SML lies at the interface between the ocean and the atmosphere, it is expected to influence the transfer of gases and particles between these compartments[6-10]. Material from the SML may become entrained in sea spray aerosol (SSA) generated by bubble bursting processes[11], but the extent of the SML's direct contribution to SSA remains unknown[12]. In the central Arctic, atmospheric particles have been found to have similar properties to particles (~100 nm diameter) in the SML beneath, suggesting that the SML may be a significant source of these aerosol particles[13]. Similarly, co-variation of anionic surfactants in aerosol and the SML in the Mediterranean suggests the SML is a source of aerosol organic matter[14]. Photochemical and heterogeneous reactions in the microlayer may also supply volatile organic compounds (VOCs) to the atmosphere, and so contribute to secondary organic aerosol formation[4, 15, 16].

The influence of the SML on air-sea exchange and marine aerosol properties is assumed to be a function of its chemical composition, but as yet, the composition of the microlayer has not been fully characterized. Relative to the underlying bulk seawater, the SML has been found to be enriched in a wide range of organic and

67 inorganic compounds ([12] and references therein; [6, 17-27]). Rising bubbles collect surface-
68 active organic material from the water column and transfer it to the microlayer[1, 2],
69 where further enrichment and/or modification (e.g. by photochemical oxidation[5], or
70 microbial degradation[1, 28]) of some compound classes may occur. Non-targeted high-
71 resolution mass spectrometry has shown a shift towards lower molecular weight
72 compounds in the SML relative to the underlying seawater, thought to be the result of
73 increased degradation[22].
74
75 The microlayer is also enriched in biogenic material that can heterogeneously
76 nucleate ice[29]. The presence of ice nucleating particles (INPs) in bulk seawater and
77 marine air masses has long been known[30-35], and recent studies indicate that the oceans
78 are probably an important source of aerosolized atmospheric INPs, particularly in
79 remote regions away from terrestrial sources[29, 36-38]. Depending on the exact nucleation
80 pathway, heterogeneous ice nucleation by INPs can raise the temperature and/or
81 lower the relative humidity at which ice crystals form in clouds, with consequent
82 impacts on cloud lifetime, precipitation and cloud radiative properties. The identity of
83 INPs in the SML, and the factors governing their abundance, remain unknown.
84
85 In this work, low mass resolution liquid chromatography mass spectrometry was used
86 to explore the molecular composition of dissolved organic matter (DOM) isolated
87 from Arctic SML and underlying seawater, with the aim of identifying features which
88 related to ice nucleation activity, an atmospherically relevant property. A combination
89 of high-mass resolution mass spectrometric techniques was then used to examine
90 these features further. The work was conducted as part of the Aerosol-Cloud Coupling
91 and Climate Interactions in the Arctic (ACCACIA) project.

Experimental section

Sample collection

Samples were collected from the Greenland and Barents Seas during cruise JR288 of the RRS *James Clark Ross* in July-August 2013. Water sampling locations are shown in Figure 1 and further details are given in Table S1 of Supplementary Information (SI). Sea surface microlayer samples were collected using a remote controlled rotating drum type sampler deployed for approximately 40 minutes per sample[29, 39]. Sub-samples of ~1 L were taken for mass spectrometric analysis. Two sampling blanks ('boat blanks') were collected by running underlying seawater from the same location over the sampler drum, and consequently through the sampler's whole collection system. Underlying seawater was collected from approximately 2-5 m depth using Niskin bottles deployed on a CTD rosette. Seawater subsamples (~10 L) were collected from the Niskin bottles into dedicated clean glass sampling bottles that were rinsed with dilute HCl (10% v/v) prior to the start of the cruise.

Atmospheric aerosol samples were collected during cruise JR288, and also during a cruise to the same area made by the RV *Lance* in March 2013. Aerosol samples were collected onto pre-combusted quartz (Whatman QM-A) filters using a high volume aerosol collector (Ecotech Hi-vol 3000; air flow ~68 m^3 hr^{-1}) fitted with a $PM_{2.5}$ size selective inlet. The sampler was located on the bridge-top deck of each ship, and automatically controlled according to wind direction in order to avoid contamination from the ship's stack. Individual samples were collected over 24 hour periods, with an average total air volume of 1261 m^3 per sample.

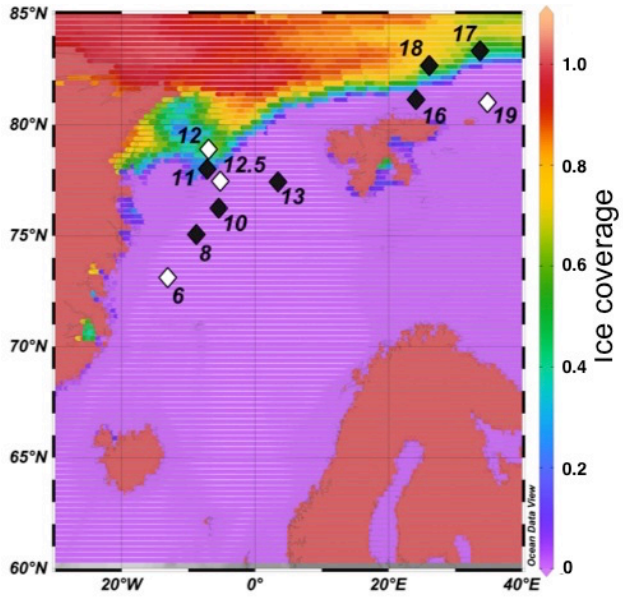

Figure 1. Locations of sea surface microlayer sampling stations during cruise JR288, superimposed on NSIDC satellite sea ice concentration data for 28 July 2013. Sea ice concentrations are shown as fractional coverage, where 0 is no ice and 1 is complete cover; values >1 are masks for land and missing data. White station symbols indicate locations where the microlayer had particularly high relative ice nucleation activity, based on median freezing temperatures, T_{50}. Figure produced using Ocean data View [40].

Sample preparation

Immediately following collection, all seawater and microlayer samples were filtered under vacuum through pre-combusted (5 hours at 450˚C) Whatman GF/F filters (nominal pore size 0.7 μm). Dedicated acid washed glass bottles and a polycarbonate filter holder were used; all were acid rinsed at least every few days. Dissolved organic matter was isolated from the filtrate by solid phase extraction (SPE) onto Agilent

136 Bond Elut PPL cartridges, using LC-MS grade solvents (Fisher Optima), according to
137 the method of Dittmar et al[41]. Procedural blanks were prepared by replacing the
138 sample with ~5 mL of rinse solution (0.01M hydrochloric acid). The operationally
139 defined fraction of the DOM isolated by this procedure is referred to as SPE-DOM.
140 SPE extraction efficiency was not evaluated here, but a previous comparison of
141 sorbents found the protocol adopted here to be the most efficient at extracting DOM
142 from seawater, with average recoveries of 43 and 62% for coastal and open ocean
143 waters respectively[41]. Longnecker et al[42] achieved DOM recoveries from Arctic
144 seawater of 32 to 43% using a variation of this method with two SPE extraction steps.
145
146 Methanolic extracts were stored in pre-combusted glass vials at -20 °C for return to
147 the UK. Prior to analysis, samples were evaporated to dryness using a vacuum solvent
148 evaporator (Biotage, Sweden) and redissolved in methanol-water (1:1 mixture).
149 Potential exists for organic matter to undergo molecular transformations, such as
150 trans-esterification of carboxylic acids and esters[43], and acetal and hemi-acetal
151 formation[44], in methanolic extracts. Some of these changes may occur very rapidly,
152 over timescales of minutes, and so be effectively unavoidable. During longer-term
153 storage, it has been shown that methanolic extracts may undergo proton exchange but
154 not esterification or hemiacetal formation[45]. Repeat analyses of our samples after
155 more than 12 months also suggests they are stable at -20 ºC.
156
157 Aerosol samples were foil wrapped and frozen at -20°C immediately following
158 collection for return to the UK. Aerosol material was extracted from the filters into
159 ultrapure water (Fisher LC-MS grade) by ultrasonication, and then extracted by SPE
160 as above. To allow direct comparison of seawater and aerosol SPE-DOM, the salinity

of the aqueous aerosol extracts was made up to that of seawater (~35 g L^{-1}) by adding sodium chloride prior to SPE. As aerosol loadings were very low, extracts from three or four consecutive aerosol samples of the same air mass origin (assigned using air mass back trajectories from NOAA Hysplit [46]) were combined.

Mass spectrometric analysis

High performance liquid chromatography-ion trap mass spectrometry (LC-IT-MS). The SPE-DOM sample extracts were first analyzed by LC-IT-MS using an HCT Plus ion trap mass spectrometer (Bruker Daltonics GmbH, Bremen, Germany) coupled to an Agilent 1100 series HPLC. A Pinnacle DB-C_{18} column with 5 μm particle size (Restek, 4.6 x 150 mm) was used with 0.1% (v/v) formic acid in ultrapure water (Optima LC-MS grade, Fisher, UK) and methanol (Optima LC-MS grade, Fisher, UK) mobile phases and a flow rate of 0.6 mL min^{-1}. Gradient elution was performed as follows: 0-13 minutes 20% methanol; 13-23 minutes increase to 60% methanol; 23-33 minutes, hold at 60% methanol; 33-43 minutes increase to 100% methanol; 43-50 minutes hold at 100% methanol; 50-53 minutes return to starting conditions; 53-59 minutes hold at starting conditions. Electrospray ionization was used with a source temperature of 365°C, nebulizer pressure of 70 psi and drying gas (N_2) flow rate of 12 L min^{-1}. The mass spectrometer was operated in alternating positive and negative ion mode, with a scan range of *m/z* 50 - 1000 and a target mass setting of *m/z* 150. Mass calibration was conducted using a standard containing arginine clusters (Sigma-Aldrich). The mass accuracy ranged from ~ 100 to 2000 ppm, and the mass resolution was 500 at *m/z* 200.

186 *Fourier transform ion cyclotron resonance mass spectrometry (FT-ICR-MS).* SPE-
187 DOM extracts were also analyzed by ultra-high mass resolution FT-ICR-MS with
188 electrospray ionization using a SolariX XR 9.4T instrument (Bruker Daltonics,
189 Coventry, UK). Samples were introduced by direct infusion at a flow rate of
190 120 μl hr^{-1}. The source temperature was 220 °C, the nebulizer gas (N_2) pressure was
191 1.2 bar and the drying gas flow rate was 4 L min^{-1}. Samples were analyzed separately
192 in positive and negative mode over a scan range of *m/z* 58 to 1200. Each sample was
193 analyzed twice, typically with 50 (negative mode) or 200 (positive mode) scans
194 collected per analysis. The mass resolution was ~140,000 at *m/z* 200. The instrument
195 was externally calibrated using sodium formate clusters. Negative mode FT-ICR-MS
196 spectra were internally recalibrated using the ubiquitous series of DOM anions
197 ($C_{17}H_{19}O_8^-$, $C_{18}H_{21}O_8^-$, $C_{19}H_{23}O_8^-$ etc) proposed by Kujawinski et al., 2009[47]. Positive
198 mode FT-ICR-MS spectra were internally calibrated using a combination of DOM
199 and common contaminant ions (e.g. proline, arginine, polyethylene glycol oligomers).
200 Aerosol SPE extracts were screened for selected ions using FT-ICR-MS in negative
201 mode, with conditions as above. Due to a lack of suitable ions, internal mass
202 calibration was not carried out for these samples.
203
204 Bulk compositional analysis was conducted for FT-ICR-MS data collected in the
205 negative mode, as this has been more widely reported in comparable previous studies.
206 Only *m/z* values that satisfied the following criteria were considered: (i) absent from
207 the procedural extraction blank (at a signal to noise ratio of at least four); (ii) present
208 in both analytical replicates; (iii) signal-to-noise ratio greater than ten. Molecular
209 formulae were generated using the SmartFormula functionality within DataAnalysis
210 4.1 software (Bruker Daltonics, Bremen, Germany), In addition to C, H and O, the

211 heteroatoms N, S and P were allowed, with a formula error limit of 1 ppm. Elemental
212 combinations were restricted according to rules adopted from similar previous work [22, 48-54], see SI for further details.
213
214
215 *High-performance liquid chromatography - quadrupole time-of-flight mass*
216 *spectrometry (LC-TOF-MS^2).* A subset of microlayer and seawater extracts were
217 analyzed by LC-TOF-MS^2 using a maXis 3G mass spectrometer (Bruker Daltonics,
218 Coventry, UK) coupled to a Dionex ultimate 3000 HPLC system (Thermo Scientific
219 Inc., UK). The column, mobile phases and gradient program were the same as those
220 used for LC-IT-MS analysis (see above), with the exception that HPLC grade water
221 (Fisher, UK) was used instead of LC-MS grade water. Differences in instrument
222 plumbing resulted in a slight retardation of retention times of ~2 minutes.
223 Electrospray ionization was used with a source temperature of 350°C, nebulizer
224 pressure of 4 bar and drying gas (N_2) flow rate of 9 L min^{-1}. Samples were analyzed in
225 positive and negative mode separately; in each mode external mass calibration was
226 conducted using Agilent low concentration tuning mix (part no. G1969-85000).
227 Fragmentation spectra for specified ions were acquired across a range of collision
228 energies (7-40 eV) in order to obtain good fragmentation spectra for as many ions as
229 possible.
230
231 The purpose of the LC-TOF-MS^2 analysis was to allow high confidence assignment
232 of molecular formulae to selected ions of interest identified by LC-IT-MS. This was
233 achieved in two ways. Firstly, it provided more accurate *m/z* values for ions of interest
234 for which the retention time was known, so constrained the number of corresponding
235 peaks in the FT-ICR-MS spectra. FT-ICR-MS spectra of microlayer samples,

236 seawater samples and procedural blanks within this narrower *m/z* window were then
237 compared to identify ions present at appropriate relative abundances, and possible
238 molecular formulae for these were generated. Secondly, possible formulae for
239 fragment ions and constant neutral losses detected by LC-TOF-MS^2 were used to
240 identify relationships between groups of ions and inform formula selection. This
241 information was combined with the FT-ICR-MS results in order to deduce probable
242 molecular formulae for the target ions.
243
244 **Supporting parameters**
245 The measurement of ice nucleating particles (INP) in untreated SML samples is
246 described in Wilson et al., 2015. In order to determine whether INP were retained
247 during the SPE extraction (Section 2.2), INP assays were also conducted on SML
248 extracts that had been dried and reconstituted in a salt-water matrix (35 g L^{-1}) and a
249 matrix blank. The reconstitution volume was selected such that analyte concentrations
250 were returned to those in the original, untreated SML sample. This allowed direct
251 comparison of the extract IN activity with the microlayer IN activity measured in the
252 raw samples during cruise JR288 [29].
253
254 Total organic carbon content of untreated SML samples was measured using a
255 Shimadzu TOC-V analyzer, as described in Wilson et al., 2015. A suite of trace gases
256 (DMS, halocarbons, monoterpenes) were measured by purge-and-trap gas
257 chromatography mass spectrometry using the method described in [55], though we
258 caution that these results are semi-quantitative at best because microlayer sampling
259 methods were not gas-tight.
260

Results and discussion

Presence of microlayer enhanced ions revealed by LC-IT-MS

Low mass resolution LC-IT-MS analysis of all samples revealed differences in organic composition, both between seawater and microlayer extracts, and within the subset of microlayer extracts. Total ion chromatograms obtained using LC-IT-MS showed a broad peak between 18 and 36 minutes in seawater and microlayer samples, while procedural blanks did not (Figs S1a, S2a). This broad peak is thought to be due to a large number of co-eluting, organic compounds present at low concentrations[56]. For some, but not all microlayer samples, discreet peaks appeared superimposed upon the broader hump (Figs S1a, S2a), suggesting a small number of ions either present at elevated levels, or with substantially higher ionization efficiencies. Base peak chromatograms (which display the abundance of the most intense ion in the mass spectra at each time point) confirmed the enhancement of selected ions in the microlayer (Figs S1b, S2b). In contrast, seawater samples did not exhibit any discreet peaks within this region.

Average mass spectra calculated for the 18-36 minute retention time region showed a characteristic distribution of peaks separated by 14 Da (corresponding to a CH_2 unit) for all seawater samples (Fig S3). Note that the choice of instrumental parameters (e.g. target mass) will influence the shape and center of the *m*/*z* distributions obtained, as well as the response factors of individual ions, so only data obtained under the same conditions can be directly compared. Average mass spectra were strikingly similar for all seawater samples, suggesting homogeneity in the extracted organic matter between sampling stations. Average mass spectra of microlayer samples

displayed additional peaks with higher relative intensity than observed in the seawater samples (Fig S3). This is consistent with the presence of elevated concentrations of certain ions in the microlayer compared to the underlying seawater.

LC-IT-MS chromatograms for microlayer sampling boat blanks did not contain these enhanced species, and the average mass spectra appeared similar to those for the seawater from which they were prepared (Figs S1, S2 and S3), suggesting they were not the result of contamination during microlayer sampling.

Inspection of base peak chromatograms and average mass spectra obtained by LT-IT-MS found 33 negative ions and 117 positive ions that were enhanced in microlayer samples, and these ions were selected for further study. Peak areas (obtained from extracted ion chromatograms) for these microlayer enhanced ions were normalized according to aqueous extraction volume, and used as a proxy for their relative abundances. As the sensitivity of ESI-MS varies across different compounds and as a function of matrix, peak areas are only used to compare the same ions (at same retention time and so approximately same matrix) across samples, and not to compare abundances of different ions within or between samples.

Link between abundance of microlayer enhanced ions and ice nucleation activity

The microlayer samples had higher ice nucleation (IN) activity than the underlying seawater, and this varied between stations (see Wilson et al., 2015). Ice nucleation ability, quantified in terms of median freezing temperature (T_{50}; the temperature at which 50% of droplets had frozen), was correlated with the relative abundances of some of the microlayer enhanced ions identified by LC-IT-MS analysis (Fig 2, Table

311 1). Considering the microlayer samples only, linear correlation coefficients of $R^2 >$
312 0.5 were obtained for 7 negative ions and 27 positive ions (Table 1); for ease, these
313 ions are referred to as 'IN tracer ions' hereafter. To examine this relationship over a
314 wider linear range, correlation analysis was extended to include the measured IN
315 activity of diluted microlayer samples (1% and 10% by volume) and calculated ion
316 abundance, assuming that peak area scales linearly for the ions of interest. This
317 revealed strong exponential relationships between IN activity and IN tracer ion
318 relative abundance, with correlation coefficients of $R^2 > 0.8$ in all but one case (Fig 2,
319 Table 1). Seawater samples also appear to broadly fit this relationship (Fig 2), but
320 were not included in quantitative correlation analysis as both ice nucleation ability
321 and peak area were at or very close to the limit of detection.
322

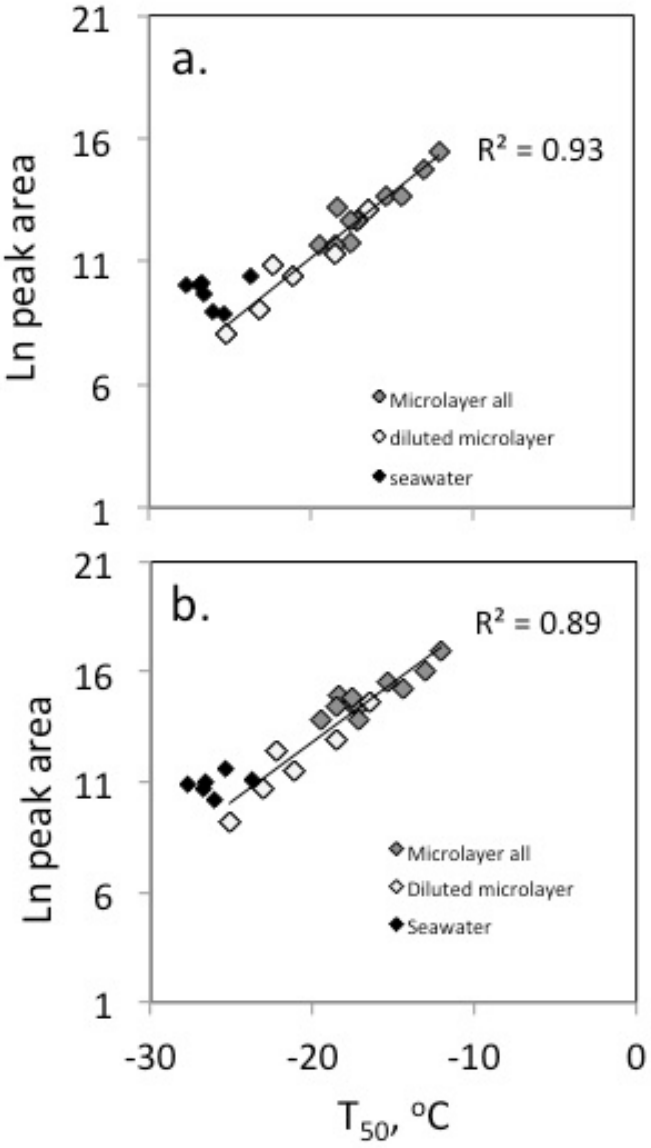

323

324

325 **Figure 2.** Natural log of volume normalized peak area plotted against 50% freezing
326 temperature, for ions with (a) retention time 30.8 mins, $[M\text{-}H]^-$ = 289.2 and (b)
327 retention time 38.5 mins, $[M+H]^+$ = 285.2 for microlayer (grey diamonds) and
328 seawater (black diamonds) samples, and microlayer samples diluted with ultrapure
329 water to 10 and 1% by volume (white diamonds). Lines of best fit and correlation
330 coefficients are for microlayer (whole and diluted) only, assuming peak area scales

linearly with sample dilution; seawater values were excluded from correlation analysis as they were at or close to the limit of detection for both ice nucleation ability and peak area.

The correlations between IN tracer ion abundance and T_{50} for microlayer samples are comparable or greater than that identified between T_{50} and TOC content of the microlayer ($R^2 = 0.51$). For many ions, the relationship between ion abundance and IN activity was also stronger than that between ion abundance and TOC (Table 1). The IN tracer ions were variably correlated with TOC (Table 1), consistent with compositional differences between the SML samples, rather than solely a homogenous DOC pool present at varying concentrations.

IN assays of reconstituted SPE extracts yielded freezing curves that were very similar to those of the salt-water matrix (Fig. S4) and of the fresh seawater analyzed immediately following collection[29]. The elevated freezing temperatures characteristic of the raw microlayer samples[29] were not observed in the reconstituted SPE extracts. This implies that the INPs are not extracted and/or preserved by the SPE protocol, and that the IN tracer ions are only associated with INPs, but do not contribute directly to ice nucleation.

355 **Table 1.** Formula assignment, correlation coefficients (R^2) and enrichment factors (EF) for ice nucleation tracer ions that were enhanced the
356 SML, in order of retention time (t_R).

t_R, mins	**Mode**	**Exact m/z**	**Suggested formula**	**Formula error, ppm**	**Adduct**	**Fragment ions**	**R^2 Peak area vs. T_{50}**	**R^2 Ln(peak area) vs. T_{50}***	**R^2 Peak area vs. TOC**	**EF range**
23.1	+	187.09647	$C_9H_{14}O_4$	0.08	$[M+H]^+$	b	0.56	0.87	0.62	12 - 436
23.9	+	273.13086	$C_{11}H_{22}O_6$	-0.00	$[M+Na]^+$	a	0.52	0.85	0.56	16 - 85
24.3	+	197.11723	$C_{11}H_{16}O_3$	-0.05	$[M+H]^+$	179.11, 161.10, (135), 133.10, 107.09, 93.07	0.55	0.84	0.85	29 - 1502
26.5	-	261.13429	$C_{12}H_{22}O_6$	-0.27	$[M-H]^-$	187.09, 125.09	0.52	0.85	0.52	2 - 175
28.6	+	285.13105 285.16727	$C_{12}H_{22}O_6$ $C_{13}H_{26}O_5$ $C_{19}H_{25}S^+$	-0.65 -0.09 -0.43	$[M+Na]^+$ $[M+Na]^+$	a	0.58	0.81	0.26	8 - 167
29.4	+	125.09606	$C_8H_{12}O$	0.25	$[M+H]^+$	a	0.61	0.90	0.55	6 - 97
29.7	+	299.14675	$C_{13}H_{24}O_6$	-0.80	$[M+Na]^+$	73.6079	0.56	0.80	0.26	14 - 101
29.9	+	123.11685	C_9H_{14}	-0.19	$[M+H]^+$	b	0.58	0.81	0.46	18 -124

30.7	+	273.13086 273.16968	$C_{11}H_{22}O_6$ $C_{14}H_{24}O_5$	0.00 -0.11	$[M+Na]^+$ $[M+H]^+$	c	0.58	0.86	0.48	6 - 50
30.8	-	289.15757 289.16557	$C_{14}H_{27}O_4P$ $C_{14}H_{26}O_6$	0.61 -0.31	$[M-H]^-$ $[M-H]^-$	215.12	0.71	0.93	0.50	5 - 115
31.0	+	315.17790	$C_{14}H_{28}O_6$	-0.30	$[M+Na]^+$	a	0.52	0.81	0.42	28 - 272
31.5	-	187.13382	$C_{10}H_{20}O_3$	-0.46	$[M-H]^-$	167.10, 151.04, 141.12, 112.98	0.56	0.87	0.53	35 - 647
31.6	+	171.13797	$C_{10}H_{18}O_2$	-0.08	$[M+H]^+$	153.13, 135.12, 107.09	0.55	0.86	0.54	12 - 266
31.7	+	273.16968	$C_{14}H_{24}O_5$	-0.11	$[M+H]^+$	153.13, 135.12	0.57	0.81	0.39	11 - 399
31.8	-	289.15757 289.16557	$C_{14}H_{27}O_4P$ $C_{14}H_{26}O_6$	0.61 -0.31	$[M-H]^-$ $[M-H]^-$	215.12, 197.11	0.61	0.86	0.46	23 - 894
31.9	+	257.17489	$C_{14}H_{24}O_4$	-0.60	$[M+H]^+$	211.08, 147.12, 137.13, 95.09	0.52	0.82	0.60	3 - 326
33.9	+	187.13281	$C_{10}H_{18}O_3$	0.33	$[M+H]^+$	173.12, 155.11, 137.10, 119.09, 109.10, 95.09	0.53	0.86	0.57	41 - 744
34.0	+	241.14100	$C_{11}H_{22}O_4$	-0.12	$[M+Na]^+$	209.12	0.54	0.81	0.41	82 - 1952
35.7	+	241.14100	$C_{11}H_{22}O_4$	0.12	$[M+Na]^+$	209.12	0.58	0.85	0.68	15 - 273
36.6	+	167.14304	$C_{11}H_{18}O$	0.19	$[M+H]^+$	149.13, 121.10, 109.10, 95.09, 81.07	0.57	0.87	0.72	162 -

										5512
36.7	-	201.14952	$C_{11}H_{22}O_3$	0.49	$[M-H]^-$	155.14	0.55	0.87	0.69	386 - 12931
36.7	+	149.13246	$C_{11}H_{16}$	0.11	$[M+H]^+$	121.10, 109.10, 107.09, 95.09	0.56	0.87	0.69	17 - 625
36.7	+	185.15361	$C_{11}H_{20}O_2$	-0.02	$[M+H]^+$	167.14, 149.13, 121.10, 109.10, 95.09, 83.09, 81.07	0.56	0.87	0.71	86 - 1927
38.5	+	285.20581	$C_{16}H_{28}O_4$	0.79	$[M+H]^+$	b	0.66	0.89	0.53	17-67
39.1	+	125.13251	C_9H_{16}	-0.26	$[M+H]^+$	c	0.52	0.87	0.67	9 - 114
39.2	-	236.11384	$C_{20}H_{42}O_8S_2$	-0.85	$[M-2H]^{2-}$	375.24, 96.96	0.64	0.84	0.29	52 - 1944
40.1	-	236.11384	$C_{20}H_{42}O_8S_2$	-0.85	$[M-2H]^{2-}$	375.24, 195.13, 154.06, 96.96	0.64	0.78	0.16	25 - 3728
40.7	+	257.17464	$C_{14}H_{24}O_4$	-0.37	$[M+H]^+$	201.15, 183.14, 165.13, 147.12, 137.13, 123.12, 95.09	0.53	0.84	0.49	8 - 244

Where two different *m/z* are listed, it was not possible to unambiguously identify the tracer ion in the FT-ICR-MS spectra. Where fragment ions are not given either (a) the ion did not fragment, (b) the fragmentation spectra were of very low intensity, or (c) the tracer ion was not apparent in the LC-TOF-MS^2 chromatogram. Rows shaded grey indicate formulae that are related to each other by the loss or gain of water molecules, so may indicate adducts of the same compound. Correlation coefficients are shown for relative abundance versus ice nucleation ability, measured as median freezing temperature (T_{50}), and total organic carbon content (TOC). *Correlation of Ln(peak area) against T_{50} includes diluted microlayer

362 samples. Enrichment factors are estimated as the ratio of the peak area in a microlayer sample to that in the corresponding seawater sample,
363 following adjustment for extraction volume; the range for all microlayer samples is shown.

Identity and potential origin of IN tracer ions

Microlayer enhanced peaks (and high IN activity) were particularly common and abundant at station 12, and also stations 6, 12.5 and 19 (Figs S1, S2 and S3). The underlying water at stations 6, 12, 12.5 and 19 did not exhibit any distinctive features in either total or size-segregated chlorophyll concentrations (C. Hughes, University of York, unpub. data), or the chlorophyll contribution of individual phytoplankton groups derived from pigment analysis (A. Small, Oxford University, unpub. data). Similarly, there was no apparent relationship between the variation in SML composition (as determined here) or freezing temperature (as presented in Wilson et al.[29]) and the numbers of bacteria present (cell count data presented in Wilson et al.[29]). Examination of temperature-salinity profiles, and the shipboard wind speed and ambient light levels at the time of sampling, and in the 6 and 24 hours prior to the SML sampling, also failed to show any corresponding trends. Interestingly, semi-quantitative determinations of the biogenic trace gases dimethyl sulfide, methyl iodide, bromochloromethane and di-iodomethane revealed that these gases also tended to be present at higher levels in microlayer samples 6, 12, 12.5 and 19 than in other samples (Fig S5). These stations were also unusual in that ethyl and propyl iodide were observed. From the above consideration of the available supporting evidence, a single factor associated with the relative abundance of IN tracer ions (and high INPs themselves) cannot be identified, but the associations with TOC and biogenic trace gases point towards a biological and/or photochemical influence.

The nature of marine INPs has not yet been fully elucidated, but evidence suggests they originate from marine phytoplankton or bacteria[60-64]. Phytoplankton cell exudates and/or cellular fragments, and the bacterial populations sustained by this material,

389 have both been suggested as possible sources[29, 36, 63]. Laboratory mesocosm
390 experiments found that peaks in airborne IN activity coincided with increases in
391 relatively aliphatic rich, low O/C organic material in submicron SSA; these changes
392 were ascribed to phytoplankton cell lysis under conditions of relatively low bacterial
393 lipase activity[36, 64, 65]. Cell breakage may occur in the surface ocean, with subsequent
394 concentration of the products in the SML, or the process may be enhanced in the SML
395 itself. Enrichments of mannose and arabinose in the SML have previously been
396 attributed to phytoplankton cell degradation[66]. Aller et al.[67] observed an increased
397 proportion of membrane damaged cells in the SML, and suggested this might be due
398 to the increased potential for viral infection, zooplankton grazing and physical
399 stresses in the microlayer. Either process could potentially result in increased
400 abundances of INPs and other biogenic material in the SML. We hypothesize that the
401 IN tracer ions originate from a phytoplankton exudate mix (including any associated
402 bacteria and viruses), of which larger sized constituents confer the IN activity.
403
404 Phytoplankton are known to release a wide variety of organic compounds, ranging in
405 size from volatile gases of less than 100 Da to macromolecules and colloids of several
406 1000 Da. As a result of sample processing and instrumental constraints, this study
407 (and all others using similar approaches), considers only an operationally defined
408 fraction of the total organic matter present. Specifically, the analytical approaches
409 used here have targeted compounds that are low molecular weight (<1000 *m/z*), water
410 soluble, neither strongly hydrophobic or strongly hydrophilic, and easily ionizable by
411 electrospray. High-resolution mass spectrometry was used to elucidate molecular
412 formulae for the IN tracer ions (Table 1). Searches of online databases (e.g.
413 Chemspider, MassBank, NIST) typically returned tens of structural isomers per

414 formula or more. Our data is insufficient to distinguish between these isomers, so we
415 can only explore whether the IN formulae are consistent with algal exudates. For
416 example, known algal metabolites with similar carbon numbers to the IN tracer ions
417 include polyunsaturated aldehydes (PUAs; e.g. decatrienal, $C_{10}H_{14}O$)[68] and
418 unsaturated hydrocarbons (e.g. fucoserratene, C_8H_{12}; dictyopterenes, $C_{11}H_{18}$)[69]. Two
419 tracer ion formulae exactly match those of compounds from these classes: isomers of
420 $C_8H_{12}O$ include the PUA octadienal, while those of $C_{11}H_{16}$ include the algal hormone
421 hormosirene[70]. Other tracer ions have formulae consistent with oxygenated organics
422 (e.g. $C_8H_{14}O_3$, $C_{12}H_{16}O_3$) formed when PUAs are produced by the cleavage of higher
423 molecular weight polyunsaturated fatty acids (PUFA)[71]. PUAs are mainly produced
424 by diatoms, as a response to cell wounding, for example by zooplankton grazing [72];
425 the elevated levels of DMS (and potentially halocarbons) observed in the samples
426 with high levels of the IN tracer ions are indicative of grazing having taken place at
427 these locations[73]. It is beyond the scope of this work to prove that the IN tracer ions
428 were indeed derived from PUAs, but we speculate that cellular damage (e.g. by
429 grazing, stress or viral infection) could cause the simultaneous release of PUAs, trace
430 gases and INPs.
431
432 The IN tracer ions were massively enriched in the SML, with enrichment factors
433 ranging from ~2 to 12931 (Table 1). Such EF values are several orders of magnitude
434 greater than observed for dissolved organic carbon and other organic molecules [12],
435 supporting the possibility that the tracer ions were formed *in-situ*. One possible
436 mechanism for this is the photo-chemical modification of organic matter within the
437 SML. Many have formulae consistent with fatty acid and dicarboxylic acid groups,
438 e.g. saturated oxo-fatty acids ($C_nH_{2n-2}O_3$), and unsaturated dicarboxylic acids (C_nH_{2n-}

$_4O_4$), which have been tentatively identified in nascent see spray aerosol[74]. Compounds of these classes, including nine with identical formulae to the IN tracer ions, have been found to increase in abundance following the irradiation of cellular material from freshwater aquatic biofilms[75]. More generally, the photochemical production of low molecular weight, saturated and unsaturated, carbonyl compounds has been demonstrated in natural microlayer samples and model systems[4, 5, 16, 76]. Alternative oxidation mechanisms include the oxidation of unsaturated organic compounds by ozone at the air-sea interface[77], or bacterial metabolism in the SML[1, 28]. Formation of the IN tracer ions within the SML by abiotic reactions or bacterial breakdown is not incompatible with a link to phytoplankton described above, as this may supply the precursor material.

Semi-quantitative comparison of seawater and microlayer SPE-DOM composition using FT-ICR-MS

Mass spectra obtained using the high resolution FT-ICR-MS echoed the general trends suggested by the LC-IT-MS analysis, described earlier. Seawater samples were similar across stations, even at the fine scale. The negative mode high-resolution mass spectra for seawater samples visually resemble those obtained in other studies[22, 47, 57, 58]. As mentioned earlier, it should be noted that relative ion intensities across the *m/z* range scanned are in part a function of user selected instrument settings. Previous studies have also reported a high level of homogeneity between SPE-DOM mass spectra for surface seawater samples[57, 58].

In contrast, SML samples displayed differences both from seawater and each other, but boat blanks were very similar to those for seawater (Fig S6). The SML spectra

464 tended to contain peaks across a wider *m/z* range than the seawater spectra, and have
465 more high intensity spikes. In the negative mode, higher molecular weight peaks (*m/z*
466 ~700 to 900) were particularly prominent in SML samples 6 and 12.5, which also had
467 high IN activity.
468
469 The visual contrast between seawater and SML spectra resembles the differences
470 observed between ESI-FT-ICR mass spectra of underlying seawater and SML from an
471 estuary, where enhancement of surfactant peaks has been observed[22]. Interestingly,
472 seawater samples incubated with different microbial communities have also been
473 shown to exhibit comparable differences in low molecular weight DOM
474 composition[59]. In that study, plankton larger than ~1 μm were removed from
475 seawater, resulting in a microbial community dominated by heterotopic bacteria.
476 High-resolution mass spectra from these incubations revealed the presence of unique,
477 high-abundance ions that were not present in spectra from whole water, and overall
478 had higher average H/C ratios and lower DBE values[59]. In light of these findings, it
479 seems plausible that differences in the DOM composition of the microlayer relative to
480 seawater observed here could, at least in part, reflect the differing microbial
481 communities in each.
482
483 In the positive mode LC-IT-MS average spectra, there is some indication that the
484 microlayer may be depleted in compounds at the higher molecular weight end of the
485 detection envelope (*m/z* 200-400; Fig S2) relative to seawater. This is in agreement
486 with the shift to smaller molecular size in the microlayer observed by Lechtenfeld et
487 al.[22], which was attributed to photochemical and microbiological degradation.
488 Meanwhile, negative mode FT-ICR-MS spectra obtained by direct injection also

489 suggested the presence of additional higher molecular weight (*m/z* ~700 to 900) peaks
490 in some SML samples that were absent from seawater (Fig S6). These peaks were not
491 present in the LC-IT-MS average mass spectra (Supp info Fig S3A), probably because
492 they have long retention times and did not elute in the time window of interest.
493
494 Assignment of molecular formulae to negatively charged ions detected by FT-ICR-
495 MS is described in the SI. Formula assignment for complex organic mixtures, where
496 multiple heteratoms must be considered, can be ambiguous[78, 79], and we consider our
497 results to be subject to uncertainty. Average DBE values and H/C ratios suggested
498 SPE-DOM from the microlayer was slightly more aliphatic than that from seawater
499 (Table S2). A tendency towards higher saturation and decreased aromaticity in the
500 microlayer relative to the underlying seawater has been observed previously[19, 22], and
501 is consistent with the enhancement of hydrophobic substances in the microlayer. That
502 the SML was more aliphatic than the underlying water, and also had higher IN
503 activity, is consistent with the observation of an association between IN activity and
504 more aliphatic material in SSA[36, 64, 65]. However, we did not observe trends in average
505 elemental rations or DBE values within the SML subset that co-varied with IN
506 activity.
507
508 **Possible occurrence of SML derived compounds in atmospheric aerosol**
509 The presence of relatively low molecular weight, highly oxygenated compounds in
510 the sea surface microlayer, raises the possibility that primary sea spray aerosol may
511 also contribute to the atmospheric aerosol burden of such compounds in the marine
512 environment. FT-ICR-MS identified ions with the same molecular formulae as five of
513 the negatively charged IN tracer ions (Table 1) in ambient atmospheric aerosol

514 sampled in the Greenland Sea during the July-August 2013, but not March 2013
515 (Table S3). Good agreement between observed spectra and simulated isotopic patterns
516 (indicated by a relatively low mSigma value) confirmed that the molecular formulae
517 agreed. These ions were absent from the aerosol sampling procedural blanks. The
518 possible occurrence of IN tracer ions in ambient atmospheric aerosol is consistent
519 with the transfer of material, possibly including INPs, from the microlayer to sea
520 spray aerosol. It has recently been demonstrated that SSA produced by wave breaking
521 contains INPs at levels in agreement with ambient INP measurements made over the
522 oceans[36]. That the IN tracer ions were only found in aerosol collected during the
523 summer, and not the early spring, is consistent with a biological source for these ions.
524
525
526

527 **Acknowledgements**

528 We acknowledge funding from the NERC ACCACIA (Aerosol-Cloud Coupling And
529 Climate Interactions in the Arctic) project (NE/I028769/1), and are grateful to the
530 Principal Investigator Prof Ian Brooks and to the cast and crew of the R/V *Lance*
531 March 2013 and JR288 July 2013 cruises. The York Centre of Excellence in Mass
532 Spectrometry was created thanks to a major capital investment through Science City
533 York, supported by Yorkshire Forward with funds from the Northern Way Initiative.
534 We thank Ed Bergström and David Ashford for assistance with FT-ICR-MS and
535 maXis LT-TOF-MS^2 analyses respectively. The authors gratefully acknowledge the
536 NOAA Air Resources Laboratory (ARL) for the provision of the HYSPLIT transport
537 and dispersion model and/or READY website (http://www.ready.noaa.gov) used in
538 this publication.
539

Supporting information. The FT-ICR-MS formula assignment procedure is described in the SI. Table S1 contains microlayer (and seawater) sampling information, and Table S2 contains average elemental composition information derived from FT-ICR-MS analysis of these samples. Table S3 provides details of aerosol sample collection, air mass origin and presence/absence of IN tracer ions. Total ion and base peak chromatograms obtained by LC-IT-MS for all samples are shown in Figures S1 and S2, and average mass spectra from these analyses are compared in Figure S3. Figure S4 shows freezing curves for reconstituted microlayer extracts, and raw microlayer and seawater extracts. Figure S5 compares the relative abundance of selected IN tracer ions with approximate concentrations of trace gases in microlayer samples. Negative mode FT-ICR mass spectra for seawater, microlayer and procedural blanks are shown in Figure S6, numbers of molecular formulae found in each sample type are given in Figure S7 (Venn diagram), and Figure S8 is a van Krevelen plot of these results. This information is available free of charge via the Internet at http://pubs.acs.org.

References

1. Cunliffe, M.; Engel, A.; Frka, S.; Gasparovic, B.; Guitart, C.; Murrell, J. C.; Salter, M.; Stolle, C.; Upstill-Goddard, R.; Wurl, O. Sea surface microlayers: A unified physicochemical and biological perspective of the air-ocean interface. *Prog. Oceanogr.* **2013,** *109*, 104-116.
2. Wurl, O.; Wurl, E.; Miller, L.; Johnson, K.; Vagle, S. Formation and global distribution of sea-surface microlayers. *Biogeosciences* **2011,** *8* (1), 121-135.
3. Sabbaghzadeh, B.; Upstill-Goddard, R. C.; Beale, R.; Pereira, R.; Nightingale, P. D. The Atlantic Ocean surface microlayer from 50 degrees N to 50 degrees S is ubiquitously enriched in surfactants at wind speeds up to 13ms(-1). *Geophys. Res. Lett.* **2017,** *44* (6), 2852-2858.
4. Ciuraru, R.; Fine, L.; van Pinxteren, M.; D'Anna, B.; Herrmann, H.; George, C. Unravelling New Processes at Interfaces: Photochemical Isoprene Production at the Sea Surface. *Environ. Sci. Technol.* **2015,** *49* (22), 13199-13205.

5. Ciuraru, R.; Fine, L.; van Pinxteren, M.; D'Anna, B.; Herrmann, H.; George, C. Photosensitized production of functionalized and unsaturated organic compounds at the air-sea interface. *Scientific Reports* **2015,** *5*.
6. Ebling, A. M.; Landing, W. M. Sampling and analysis of the sea surface microlayer for dissolved and particulate trace elements. *Mar. Chem.* **2015,** *177*, 134-142.
7. Shaw, M. D.; Carpenter, L. J. Modification of Ozone Deposition and I-2 Emissions at the Air-Aqueous Interface by Dissolved Organic Carbon of Marine Origin. *Environ. Sci. Technol.* **2013,** *47* (19), 10947-10954.
8. del Vento, S.; Dachs, J. Influence of the surface microlayer on atmospheric deposition of aerosols and polycyclic aromatic hydrocarbons. *Atmos. Environ.* **2007,** *41* (23), 4920-4930.
9. Frew, N. M.; Bock, E. J.; Schimpf, U.; Hara, T.; Haussecker, H.; Edson, J. B.; McGillis, W. R.; Nelson, R. K.; McKenna, S. P.; Uz, B. M.; Jahne, B. Air-sea gas transfer: Its dependence on wind stress, small-scale roughness, and surface films. *J. Geophys. Res.: Oceans* **2004,** *109* (C8), 23.
10. Donaldson, D. J.; George, C. Sea-Surface Chemistry and Its Impact on the Marine Boundary Layer. *Environ. Sci. Technol.* **2012,** *46* (19), 10385-10389.
11. Blanchard, D. C. Sea-to-air transport of surface active material. *Science* **1964,** *146* (364), 396-&.
12. Quinn, P. K.; Collins, D. B.; Grassian, V. H.; Prather, K. A.; Bates, T. S. Chemistry and Related Properties of Freshly Emitted Sea Spray Aerosol. *Chem. Rev.* **2015,** *115* (10), 4383-4399.
13. Leck, C.; Bigg, E. K. Biogenic particles in the surface microlayer and overlaying atmosphere in the central Arctic Ocean during summer. *Tellus Series B-Chemical and Physical Meteorology* **2005,** *57* (4), 305-316.
14. Roslan, R. N.; Hanif, N. M.; Othman, M. R.; Azmi, W.; Yan, X. X.; Ali, M. M.; Mohamed, C. A. R.; Latif, M. T. Surfactants in the sea-surface microlayer and their contribution to atmospheric aerosols around coastal areas of the Malaysian peninsula. *Marine Pollution Bulletin* **2010,** *60* (9), 1584-1590.
15. Mungall, E. L.; Abbatt, J. P. D.; Wentzell, J. J. B.; Lee, A. K. Y.; Thomas, J. L.; Blais, M.; Gosselin, M.; Miller, L. A.; Papakyriakou, T.; Willis, M. D.; Liggio, J. Microlayer source of oxygenated volatile organic compounds in the summertime marine Arctic boundary layer. *Proc. Natl. Acad. Sci. U.S.A.* **2017,** *114* (24), 6203-6208.
16. Zhou, X. L.; Mopper, K. Photochemical production of low-molecular-weight carbonyl compounds in seawater and surface microlayer and their air-sea exchange. *Mar. Chem.* **1997,** *56* (3-4), 201-213.
17. van Pinxteren, M.; Muller, C.; Iinuma, Y.; Stolle, C.; Herrmann, H. Chemical Characterization of Dissolved Organic Compounds from Coastal Sea Surface Micro layers (Baltic Sea, Germany). *Environ. Sci. Technol.* **2012,** *46* (19), 10455-10462.
18. Antonowicz, J. P. Daily cycle of variability contents of phosphorus forms in surface microlayer of a light salinity Baltic Sea Lagoon lake (North Poland) - Part II. *Central European Journal of Chemistry* **2013,** *11* (5), 817-826.
19. Calace, N.; Mirante, S.; Petronio, B. M.; Pietroletti, M.; Rugo, C. Fulvic acid enrichment in the microlayer of the Gerlache Inlet sea (Antarctica): Preliminary results. *International Journal of Environmental Analytical Chemistry* **2004,** *84* (6-7), 413-421.

20. Garcia-Flor, N.; Guitart, C.; Abalos, M.; Dachs, J.; Bayona, J. M.; Albaiges, J. Enrichment of organochlorine contaminants in the sea surface microlayer: An organic carbon-driven process. *Mar. Chem.* **2005,** *96* (3-4), 331-345.
21. Hardy, J. T.; Cleary, J. Surface microlayer contamination and toxicity in the German Bight. *Mar. Ecol. Prog. Ser.* **1992,** *91* (1-3), 203-210.
22. Lechtenfeld, O. J.; Koch, B. P.; Gasparovic, B.; Frka, S.; Witt, M.; Kattner, G. The influence of salinity on the molecular and optical properties of surface microlayers in a karstic estuary. *Mar. Chem.* **2013,** *150*, 25-38.
23. Galgani, L.; Piontek, J.; Engel, A. Biopolymers form a gelatinous microlayer at the air-sea interface when Arctic sea ice melts. *Scientific Reports* **2016,** *6*, 10.
24. Cincinelli, A.; Stortini, A. M.; Perugini, M.; Checchini, L.; Lepri, L. Organic pollutants in sea-surface microlayer and aerosol in the coastal environment of Leghorn - (Tyrrhenian Sea). *Mar. Chem.* **2001,** *76* (1-2), 77-98.
25. Jayarathne, T.; Sultana, C. M.; Lee, C.; Malfatti, F.; Cox, J. L.; Pendergraft, M. A.; Moore, K. A.; Azam, F.; Tivanski, A. V.; Cappa, C. D.; Bertram, T. H.; Grassian, V. H.; Prather, K. A.; Stone, E. A. Enrichment of Saccharides and Divalent Cations in Sea Spray Aerosol During Two Phytoplankton Blooms. *Environ. Sci. Technol.* **2016,** *50* (21), 11511-11520.
26. Gao, Q.; Leck, C.; Rauschenberg, C.; Matrai, P. A. On the chemical dynamics of extracellular polysaccharides in the high Arctic surface microlayer. *Ocean Science* **2012,** *8* (4), 401-418.
27. Kuznetsova, M.; Lee, C.; Aller, J. Characterization of the proteinaceous matter in marine aerosols. *Mar. Chem.* **2005,** *96* (3-4), 359-377.
28. Kuznetsova, M.; Lee, C. Enhanced extracellular enzymatic peptide hydrolysis in the sea-surface microlayer. *Mar. Chem.* **2001,** *73* (3-4), 319-332.
29. Wilson, T. W.; Ladino, L. A.; Alpert, P. A.; Breckels, M. N.; Brooks, I. M.; Browse, J.; Burrows, S. M.; Carslaw, K. S.; Huffman, J. A.; Judd, C.; Kilthau, W. P.; Mason, R. H.; McFiggans, G.; Miller, L. A.; Najera, J. J.; Polishchuk, E.; Rae, S.; Schiller, C. L.; Si, M.; Temprado, J. V.; Whale, T. F.; Wong, J. P. S.; Wurl, O.; Yakobi-Hancock, J. D.; Abbatt, J. P. D.; Aller, J. Y.; Bertram, A. K.; Knopf, D. A.; Murray, B. J. A marine biogenic source of atmospheric ice-nucleating particles. *Nature* **2015,** *525* (7568), 234-.
30. Bigg, E. K. Ice nucleus concentrations in remote areas. *Journal of the Atmospheric Sciences* **1973,** *30* (6), 1153-1157.
31. Bigg, E. K. Ice forming nuclei in the high Arctic. *Tellus Series B-Chemical and Physical Meteorology* **1996,** *48* (2), 223-233.
32. Schnell, R. C. Ice nuclei in seawater, fog water and marine air off the coast of Nova-Scotia - summer 1975. *Journal of the Atmospheric Sciences* **1977,** *34* (8), 1299-1305.
33. Schnell, R. C.; Vali, G. Freezing nuclei in marine waters. *Tellus* **1975,** *27* (3), 321-323.
34. Schnell, R. C.; Vali, G. Biogenic ice nuclei. 1. Terrestrial and marine sources. *Journal of the Atmospheric Sciences* **1976,** *33* (8), 1554-1564.
35. Rosinski, J.; Haagenson, P. L.; Nagamoto, C. T.; Parungo, F. Nature of ice-forming nuclei in marine air masses. *Journal of Aerosol Science* **1987,** *18* (3), 291-.
36. DeMott, P. J.; Hill, T. C. J.; McCluskey, C. S.; Prather, K. A.; Collins, D. B.; Sullivan, R. C.; Ruppel, M. J.; Mason, R. H.; Irish, V. E.; Lee, T.; Hwang, C. Y.; Rhee, T. S.; Snider, J. R.; McMeeking, G. R.; Dhaniyala, S.; Lewis, E. R.; Wentzell, J. J. B.;

Abbatt, J.; Lee, C.; Sultana, C. M.; Ault, A. P.; Axson, J. L.; Martinez, M. D.; Venero, I.; Santos-Figueroa, G.; Stokes, M. D.; Deane, G. B.; Mayol-Bracero, O. L.; Grassian, V. H.; Bertram, T. H.; Bertram, A. K.; Moffett, B. F.; Franc, G. D. Sea spray aerosol as a unique source of ice nucleating particles. *Proc. Natl. Acad. Sci. U.S.A.* **2016,** *113* (21), 5797-5803.

37. Burrows, S. M.; Hoose, C.; Poschl, U.; Lawrence, M. G. Ice nuclei in marine air: biogenic particles or dust? *Atmos. Chem. Phys.* **2013,** *13* (1), 245-267.

38. Vergara-Temprado, J.; Murray, B. J.; Wilson, T. W.; O'Sullivan, D.; Browse, J.; Pringle, K. J.; Ardon-Dryer, K.; Bertram, A. K.; Burrows, S. M.; Ceburnis, D.; DeMott, P. J.; Mason, R. H.; O'Dowd, C. D.; Rinaldi, M.; Carslaw, K. S. Contribution of feldspar and marine organic aerosols to global ice nucleating particle concentrations. *Atmos. Chem. Phys.* **2017,** *17* (5), 3637-3658.

39. Knulst, J. C.; Rosenberger, D.; Thompson, B.; Paatero, J. Intensive sea surface microlayer investigations of open leads in the pack ice during Arctic Ocean 2001 expedition. *Langmuir* **2003,** *19* (24), 10194-10199.

40. Schlitzer, R. *Ocean Data View*, http://odv.awi.de: 2014.

41. Dittmar, T.; Koch, B.; Hertkorn, N.; Kattner, G. A simple and efficient method for the solid-phase extraction of dissolved organic matter (SPE-DOM) from seawater. *Limnology and Oceanography-Methods* **2008,** *6*, 230-235.

42. Longnecker, K. Dissolved organic matter in newly formed sea ice and surface seawater. *Geochim. Cosmochim. Acta* **2015,** *171*, 39-49.

43. McIntyre, C.; McRae, C. Proposed guidelines for sample preparation and ESI-MS analysis of humic substances to avoid self-esterification. *Organic Geochemistry* **2005,** *36* (4), 543-553.

44. Bateman, A. P.; Walser, M. L.; Desyaterik, Y.; Laskin, J.; Laskin, A.; Nizkorodov, S. A. The effect of solvent on the analysis of secondary organic aerosol using electrospray ionization mass spectrometry. *Environ. Sci. Technol.* **2008,** *42* (19), 7341-7346.

45. Flerus, R.; Koch, B. P.; Schmitt-Kopplin, P.; Witt, M.; Kattner, G. Molecular level investigation of reactions between dissolved organic matter and extraction solvents using FT-ICR MS. *Mar. Chem.* **2011,** *124* (1-4), 100-107.

46. Stein, A. F.; Draxler, R. R.; Rolph, G. D.; Stunder, B. J. B.; Cohen, M. D.; Ngan, F. NOAA's HYSPLIT atmospheric transport and dispersion modeling system. *Bulletin American Meteorological Society* **2015,** *96*, 2059-2077.

47. Kujawinski, E. B.; Longnecker, K.; Blough, N. V.; Del Vecchio, R.; Finlay, L.; Kitner, J. B.; Giovannoni, S. J. Identification of possible source markers in marine dissolved organic matter using ultrahigh resolution mass spectrometry. *Geochim. Cosmochim. Acta* **2009,** *73* (15), 4384-4399.

48. Hertkorn, N.; Harir, M.; Koch, B. P.; Michalke, B.; Schmitt-Kopplin, P. High-field NMR spectroscopy and FTICR mass spectrometry: powerful discovery tools for the molecular level characterization of marine dissolved organic matter. *Biogeosciences* **2013,** *10* (3), 1583-1624.

49. Hawkes, J. A.; Hansen, C. T.; Goldhammer, T.; Bach, W.; Dittmar, T. Molecular alteration of marine dissolved organic matter under experimental hydrothermal conditions. *Geochim. Cosmochim. Acta* **2016,** *175*, 68-85.

50. Schmitt-Kopplin, P.; Liger-Belair, G.; Koch, B. P.; Flerus, R.; Kattner, G.; Harir, M.; Kanawati, B.; Lucio, M.; Tziotis, D.; Hertkorn, N.; Gebefugi, I. Dissolved organic matter in sea spray: a transfer study from marine surface water to aerosols. *Biogeosciences* **2012,** *9* (4), 1571-1582.

51. Stubbins, A.; Spencer, R. G. M.; Chen, H. M.; Hatcher, P. G.; Mopper, K.; Hernes, P. J.; Mwamba, V. L.; Mangangu, A. M.; Wabakanghanzi, J. N.; Six, J. Illuminated darkness: Molecular signatures of Congo River dissolved organic matter and its photochemical alteration as revealed by ultrahigh precision mass spectrometry. *Limnol. Oceanogr.* **2010,** *55* (4), 1467-1477.
52. Gurganus, S. C.; Wozniak, A. S.; Hatcher, P. G. Molecular characteristics of the water soluble organic matter in size-fractionated aerosols collected over the North Atlantic Ocean. *Mar. Chem.* **2015,** *170*, 37-48.
53. Kujawinski, E. B.; Behn, M. D. Automated analysis of electrospray ionization Fourier transform ion cyclotron resonance mass spectra of natural organic matter. *Anal. Chem.* **2006,** *78* (13), 4363-4373.
54. Wozniak, A. S.; Bauer, J. E.; Sleighter, R. L.; Dickhut, R. M.; Hatcher, P. G. Technical Note: Molecular characterization of aerosol-derived water soluble organic carbon using ultrahigh resolution electrospray ionization Fourier transform ion cyclotron resonance mass spectrometry. *Atmos. Chem. Phys.* **2008,** *8* (17), 5099-5111.
55. Andrews, S. J.; Hackenberg, S. C.; Carpenter, L. J. Technical Note: A fully automated purge and trap GC-MS system for quantification of volatile organic compound (VOC) fluxes between the ocean and atmosphere. *Ocean Sci.* **2015,** *11* (2), 313-321.
56. Dittmar, T.; Whitehead, K.; Minor, E. C.; Koch, B. P. Tracing terrigenous dissolved organic matter and its photochemical decay in the ocean by using liquid chromatography/mass spectrometry. *Mar. Chem.* **2007,** *107* (3), 378-387.
57. Flerus, R.; Lechtenfeld, O. J.; Koch, B. P.; McCallister, S. L.; Schmitt-Kopplin, P.; Benner, R.; Kaiser, K.; Kattner, G. A molecular perspective on the ageing of marine dissolved organic matter. *Biogeosciences* **2012,** *9* (6), 1935-1955.
58. Gonsior, M.; Peake, B. M.; Cooper, W. T.; Podgorski, D. C.; D'Andrilli, J.; Dittmar, T.; Cooper, W. J. Characterization of dissolved organic matter across the Subtropical Convergence off the South Island, New Zealand. *Mar. Chem.* **2011,** *123* (1), 99-110.
59. Kujawinski, E. B.; Longnecker, K.; Barott, K. L.; Weber, R. J. M.; Kido Soule, M. C. Microbial Community Structure Affects Marine Dissolved Organic Matter Composition. *Frontiers in Marine Science* **2016,** *3* (45).
60. Knopf, D. A.; Alpert, P. A.; Wang, B.; Aller, J. Y. Stimulation of ice nucleation by marine diatoms. *Nat. Geosci.* **2011,** *4* (2), 88-90.
61. Schnell, R. C. Ice nuclei produced by laboratory cultured marine phytoplankton. *Geophys. Res. Lett.* **1975,** *2* (11), 500-502.
62. Fall, R.; Schnell, R. C. Association of an ice-nucleating psuedomonad with cultures of the marine dinoflagellate, *Heterocapsa niei*. *J. Mar. Res.* **1985,** *43* (1), 257-265.
63. Ladino, L. A.; Yakobi-Hancock, J. D.; Kilthau, W. P.; Mason, R. H.; Si, M.; Li, J.; Miller, L. A.; Schiller, C. L.; Huffman, J. A.; Aller, J. Y.; Knopf, D. A.; Bertram, A. K.; Abbatt, J. P. D. Addressing the ice nucleating abilities of marine aerosol: A combination of deposition mode laboratory and field measurements. *Atmos. Environ.* **2016,** *132*, 1-10.
64. McCluskey, C. S.; Hill, T. C. J.; Malfatti, F.; Sultana, C. M.; Lee, C.; Santander, M. V.; Beall, C. M.; Moore, K. A.; Cornwell, G. C.; Collins, D. B.; Prather, K. A.; Jayarathne, T.; Stone, E. A.; Azam, F.; Kreidenweis, S. M.; DeMott, P. J. A Dynamic Link between Ice Nucleating Particles Released in Nascent Sea Spray Aerosol and

Oceanic Biological Activity during Two Mesocosm Experiments. *Journal of the Atmospheric Sciences* **2017,** *74* (1), 151-166.
65. Wang, X. F.; Sultana, C. M.; Trueblood, J.; Hill, T. C. J.; Malfatti, F.; Lee, C.; Laskina, O.; Moore, K. A.; Beall, C. M.; McCluskey, C. S.; Cornwell, G. C.; Zhou, Y. Y.; Cox, J. L.; Pendergraft, M. A.; Santander, M. V.; Bertram, T. H.; Cappa, C. D.; Azam, F.; DeMott, P. J.; Grassian, V. H.; Prather, K. A. Microbial Control of Sea Spray Aerosol Composition: A Tale of Two Blooms. *Acs Central Science* **2015,** *1* (3), 124-131.
66. Compiano, A. M.; Romano, J. C.; Garabetian, F.; Laborde, P.; Delagiraudiere, I. Monosaccharide composition of particulate hydrolyzable sugar fraction in surface microlayers from brackish and marine waters. *Mar. Chem.* **1993,** *42* (3-4), 237-251.
67. Aller, J. Y.; Kuznetsova, M. R.; Jahns, C. J.; Kemp, P. F. The sea surface microlayer as a source of viral and bacterial enrichment in marine aerosols. *Journal of Aerosol Science* **2005,** *36* (5-6), 801-812.
68. Miralto, A.; Barone, G.; Romano, G.; Poulet, S. A.; Ianora, A.; Russo, G. L.; Buttino, I.; Mazzarella, G.; Laabir, M.; Cabrini, M.; Giacobbe, M. G. The insidious effect of diatoms on copepod reproduction. *Nature* **1999,** *402* (6758), 173-176.
69. Stonik, V.; Stonik, I. Low-Molecular-Weight Metabolites from Diatoms: Structures, Biological Roles and Biosynthesis. *Marine Drugs* **2015,** *13* (6), 3672.
70. Prestegard, S.; Erga, S.; Steinrücken, P.; Mjøs, S.; Knutsen, G.; Rohloff, J. Specific Metabolites in a Phaeodactylum tricornutum Strain Isolated from Western Norwegian Fjord Water. *Marine Drugs* **2016,** *14* (1), 9.
71. Wichard, T.; Pohnert, G. Formation of halogenated medium chain hydrocarbons by a lipoxygenase/hydroperoxide halolyase-mediated transformation in planktonic microalgae. *Journal of the American Chemical Society* **2006,** *128* (22), 7114-7115.
72. Pohnert, G. Wound-activated chemical defense in unicellular planktonic algae. *Angewandte Chemie-International Edition* **2000,** *39* (23), 4352-+.
73. Wolfe, G. V.; Steinke, M.; Kirst, G. O. Grazing-activated chemical defence in a unicellular marine alga. *Nature* **1997,** *387* (6636), 894-897.
74. Cochran, R. E.; Laskina, O.; Jayarathne, T.; Laskin, A.; Laskin, J.; Lin, P.; Sultana, C.; Lee, C.; Moore, K. A.; Cappa, C. D.; Bertram, T. H.; Prather, K. A.; Grassian, V. H.; Stone, E. A. Analysis of Organic Anionic Surfactants in Fine and Coarse Fractions of Freshly Emitted Sea Spray Aerosol. *Environ. Sci. Technol.* **2016,** *50* (5), 2477-2486.
75. Bruggemann, M.; Hayeck, N.; Bonnineau, C.; Pesce, S.; Alpert, P. A.; Perrier, S.; Zuth, C.; Hoffmann, T.; Chen, J.; George, C. Interfacial photochemistry of biogenic surfactants: a major source of abiotic volatile organic compounds. *Faraday Discussions* **2017,** *200*, 59-74.
76. Zhou, S.; Gonzalez, L.; Leithead, A.; Finewax, Z.; Thalman, R.; Vlasenko, A.; Vagle, S.; Miller, L. A.; Li, S. M.; Bureekul, S.; Furutani, H.; Uematsu, M.; Volkamer, R.; Abbatt, J. Formation of gas-phase carbonyls from heterogeneous oxidation of polyunsaturated fatty acids at the air-water interface and of the sea surface microlayer. *Atmos. Chem. Phys.* **2014,** *14* (3), 1371-1384.
77. Hung, H. M.; Ariya, P. Oxidation of oleic acid and oleic acid/sodium chloride(aq) mixture droplets with ozone: Changes of hygroscopicity and role of secondary reactions. *J. Phys. Chem. A* **2007,** *111* (4), 620-632.

78. Kind, T.; Fiehn, O. Metabolomic database annotations via query of elemental compositions: Mass accuracy is insufficient even at less than 1 ppm. *Bmc Bioinformatics* **2006,** *7*, 10.
79. Tolić, N.; Liu, Y.; Liyu, A.; Shen, Y.; Tfaily, M. M.; Kujawinski, E. B.; Longnecker, K.; Kuo, L.-J.; Robinson, E. W.; Paša-Tolić, L.; Hess, N. J. Formularity: Software for Automated Formula Assignment of Natural and Other Organic Matter from Ultrahigh-Resolution Mass Spectra. *Anal. Chem.* **2017,** *89* (23), 12659-12665.